HortScience 60(7):1200–1207. 2025. https://doi.org/10.21273/HORTSCI18622-25

Comparative Analysis of Male and Female Floral Development in *Actinidia chinensis* and *Actinidia eriantha*

Jiaqi Dong
State Key Laboratory of Plant Diversity and Specialty Crops, Wuhan Botanical Garden, Chinese Academy of Sciences, Wuhan 430074, China; and College of Advanced Agricultural Sciences, University of Chinese Academy of Sciences, Beijing 100049, China

Linhui Wu
State Key Laboratory of Plant Diversity and Specialty Crops, Wuhan Botanical Garden, Chinese Academy of Sciences, Wuhan 430074, China; and Key Laboratory of Ministry of Education for Genetics, Breeding and Multiple Utilization of Crops, College of Horticulture, Fujian Agriculture and Forestry University, Fuzhou 350002, China

Hao Zheng, Yule Wang, Fei Han, Caihong Zhong, and Qiong Zhang
State Key Laboratory of Plant Diversity and Specialty Crops, Wuhan Botanical Garden, Chinese Academy of Sciences, Wuhan 430074, China

Keywords. flower, *FrBy*, kiwifruit, morphological differentiation, sex, *SyGl*

Abstract. **Members belonging to the genus *Actinidia* are perennial dioecious fruit trees. Variation in male and female floral organs during growth is crucial in sex determination. Previous studies have been limited to individual kiwifruit species (*Actinidia chinensis* and *Actinidia deliciosa*), and although two sex determination genes have been identified, their differential expression has not been linked to differences in pistil development. In the present study, we investigated male and female flower development in two kiwifruit species, namely, *A. chinensis* and *Actinidia eriantha*. Kiwifruit flower development was divided into seven stages. The first four stages are common to both male and female flower development in kiwifruits, and the primary stage of male and female flower development in kiwifruits begins at stage 5, which is largely reflected by the absence of development of ovule primordia in male kiwifruit, whereas differences in flower development between the two kiwifruit species are primarily in the timing of the initiation of the squaring stage, time required for the later stages of flower development (stage 6), and size of flower buds. Quantitative results demonstrated that *SyGl* was persistently and highly expressed after stage 4 in male kiwifruit flowers, possibly causing abnormal development of the pistil and ovary malformation in male kiwifruit flowers. In contrast, *FrBy* was up-regulated in male flowers of *A. chinensis* and *A. eriantha* during late developmental stages (stage 5 or stage 6), coinciding with pollen maturation. We propose that this peaked expression is linked to the programmed degradation of the anther chorionic layer, facilitating timely dehiscence and pollen maturation. Altogether, the findings of this study link the stages of kiwifruit flower development in the two species with their phenological periods and flower bud morphology, thus providing a reference for future comparison of flower development stages and gene expression during development in kiwifruits.**

Kiwifruit is a fruit crop native to China, which has been successfully cultivated from the wild since the 20th century (Huang 2022). It is a perennial deciduous vine fruit tree of the genus *Actinidia* and belongs to the Actinidiaceae family. China is the world's largest producer and importer of kiwifruit, with a huge consumer market (Zhong et al. 2021). The most commercially cultivated kiwifruit varieties are *A. chinensis*, *A. deliciosa*, *A. eriantha*, and *Actinidia arguta* worldwide (Fang et al. 2019).

All members of the genus *Actinidia*, comprising 54 species and 21 varieties, are probably functionally dioecious, with male and female flowers blooming on different plants (Huang 2016). The flowers, whether female or male plants, are morphologically fully flowered. Female plants have well-developed pistils and nonfunctional stamens with normal appearance, whereas male plants have normally developed stamens and rudimentary pistils without style and ovules. Although all floral organs in both male and female flowers initiate development, the growth of gynoecium in male flowers is arrested at an early stage of development (Brundell 1975; Polito and Grant 1984), whereas that of stamens in female flowers halts at a later stage through programmed death-mediated microspore degeneration (Coimbra et al. 2004; Falasca et al. 2013). Previous studies on the development of kiwifruit flowers have focused on *A. chinensis* and *A. deliciosa*, and more recently on *A. arguta* (Li et al. 2024); however, studies on the flower development of *A. eriantha*, another important commercially cultivated species, are sparse. Furthermore, previous studies have primarily focused on differences between males and females during late morphological differentiation; however, less attention has been paid to the study of early morphological differentiation of kiwifruit flower bud (Brundell 1975; Caporali et al. 2019; Li et al. 2024).

The kiwifruit sex system is an active Y-type system involving two intricately linked dominant genes: one suppresses pistil development (SuF), and another promotes anther maturation (M) (Huang 2016; Westergaard 1958). At present, sex-linked markers have been developed for different species of kiwifruit (De Mori et al. 2022; Guo et al. 2023; Liu et al. 2016). In addition, male-specific Y-linked regions have been identified in four kiwifruit genomes (Akagi et al. 2023). Furthermore, two sexed kiwifruit genomes have been assembled and annotated (Han et al. 2023; Tahir et al. 2022). Nevertheless, the precise molecular mechanism underlying sex determination in kiwifruits and factors responsible for the observed differences in flower development between male and female kiwifruits remains unclear.

Zhang et al. (2015) used a population of interspecific crosses between *A. rufa* and *A. chinensis* and successfully identified the sex-determining region in kiwifruit as a 1-Mb subtelomeric region on chromosome 25. Recently, Akagi et al. (2018) used a combination of genome-wide cataloging and transcriptome sequencing to further narrow down the male-specific region on kiwifruit chromosome 25 to ~0.49 Mb. This approach identified a male-specific gene encoding a C-type cytokinin-responsive factor. This factor is specifically expressed at the early stages of development of male flower gynoecium and has been demonstrated to suppress carpel development. Further analysis of differentially expressed genes in the

Table 1. Primers used for quantitative reverse transcription polymerase chain reaction analysis.

Gene	Sequence for primers
SyGl	F: 5′-ATTTGTATTGCTCTGGTGCTT-3′
	R: 5′-ACTTCCATGCCTCTTAGCTC-3′
FrBy	F: 5′-AACCAACACTCGCCTTCCCA-3′
	R: 5′-GGATGGGTGATAGGAGAGGCATC-3′
Actin	F: 5′-TGAGAGATTCCGTTGCCCAGAAGT-3′
	R: 5′-TTCCTTACTCATGCGGTCTGCGAT-3′

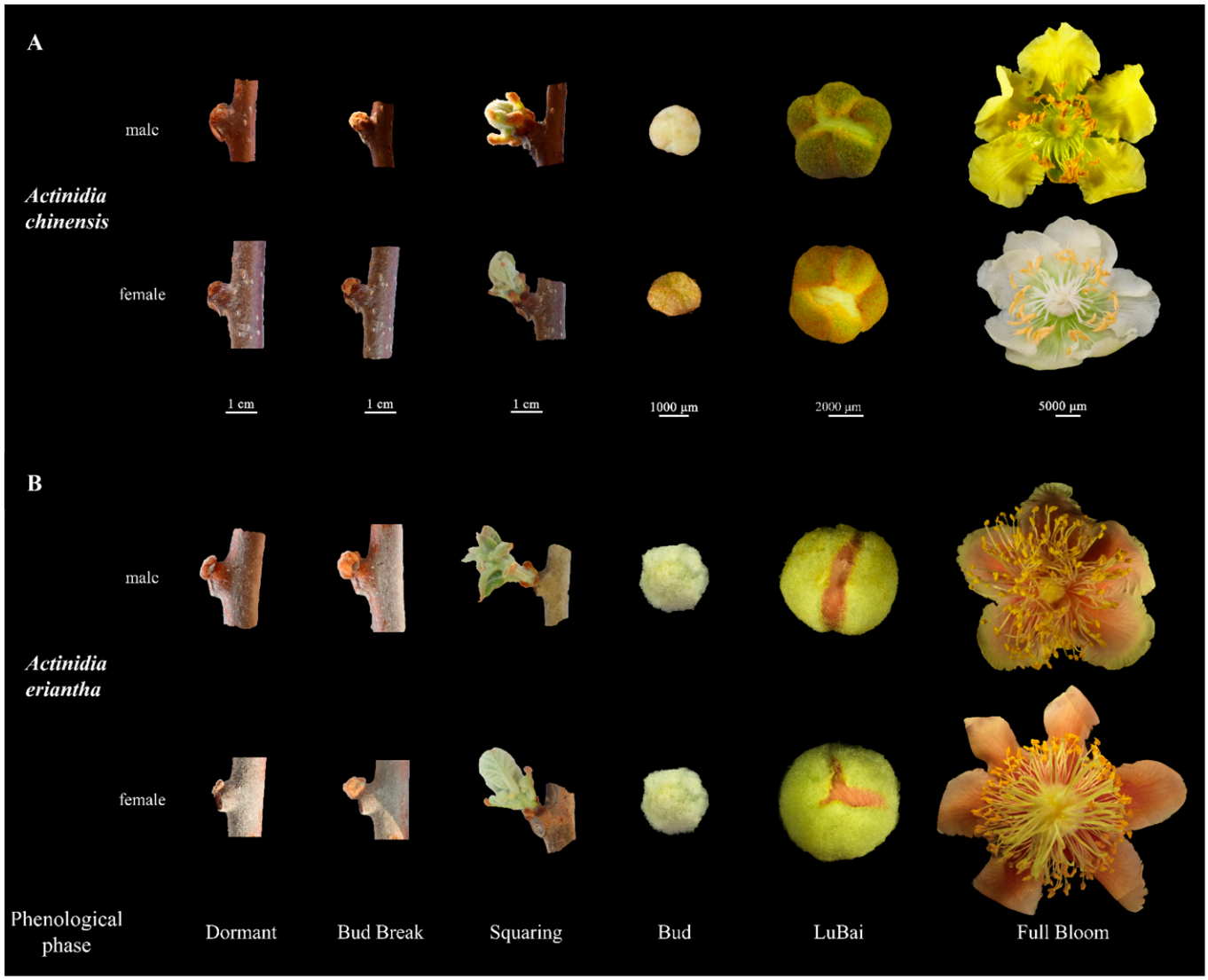

Fig. 1. Morphological changes in male and female of *Actinidia chinensis* (**A**) and *Actinidia eriantha* (**B**) during flowering.

stamens of male and female flowers identified a gene belonging to the MTR1 family, facilitating the degradation of the tapetum to maintain pollen fertility. The gene is specifically expressed in the early stages of development of the stamens in male flowers (Akagi et al. 2019). Despite the identification of two key sex-determining genes in kiwifruit, the potential contribution to the observed differences in male and female flower development as well as the mechanisms through which they exert their effects remain elusive.

At present, little research has been conducted on the differences between male and female flower differentiation in kiwifruit. Certain studies have demonstrated that similar to the flower bud development of other fruit trees, the flower bud development of male and female flowers of kiwifruit proceeds from the outside to the inside in the order of sepals, petals, stamens, and pistils (Liu 1997). Wang et al. (2001) studied the morphological differences in flower bud differentiation in *Actinidia kolomikta* and found that differences in the morphology between male and female flowers occur after the differentiation of gynoecium primordium. Studies on flower organ fertility in *A. chinensis* and *A. arguta* have demonstrated that gynoecium sterility in male flowers is attributed to the arrested development of ovule primordium, whereas anthers in female flowers are aborted due to abnormal metabolism of the tapetum, causing microspore abortion in the female plant (Li and Liu 2016; Yang et al. 2011).

Although the development of male and female flower organs in kiwifruits has been studied at the cytological level, the overall developmental stages have not been comprehensively elucidated. In the present study, we observed and compared the changes at the developmental stages in *A. chinensis* and *A. eriantha* flowers and elucidated the expression of sex-determining genes during flower development, paving the way to elucidating the regulatory network underlying sex differentiation in kiwifruit.

Materials and Methods

Plant material and cultivation conditions. The experimental site (30°33′N, 114°25′E) was located at the Wuhan Botanical Garden, Chinese Academy of Sciences, Wuhan, China. Kiwifruit over 3 years of age without pests and diseases were studied. The experimental plants were grown and maintained with routine pruning and watering and fertilizer addition.

Received for publication 26 Mar 2025. Accepted for publication 29 Apr 2025.
Published online 27 Jun 2025.
This research was funded by the earmarked fund for the China Agriculture Research System (CARS-26), Hubei Hongshan Laboratory (2021HSZD017), Science Fund for Creative Research Groups of the Natural Science Foundation of Hubei Province (2024AFA035), the Key R&D Program of Shaanxi Province (2023-ZDLNY-24), and Hubei Key Laboratory of Germplasm Innovation and Utilization of Fruit Trees (GSSZ202301).
C.Z. and Q.Z. are the corresponding authors. E-mail: zhongch@wbgcas.cn and qiongzhang@wbgcas.cn.

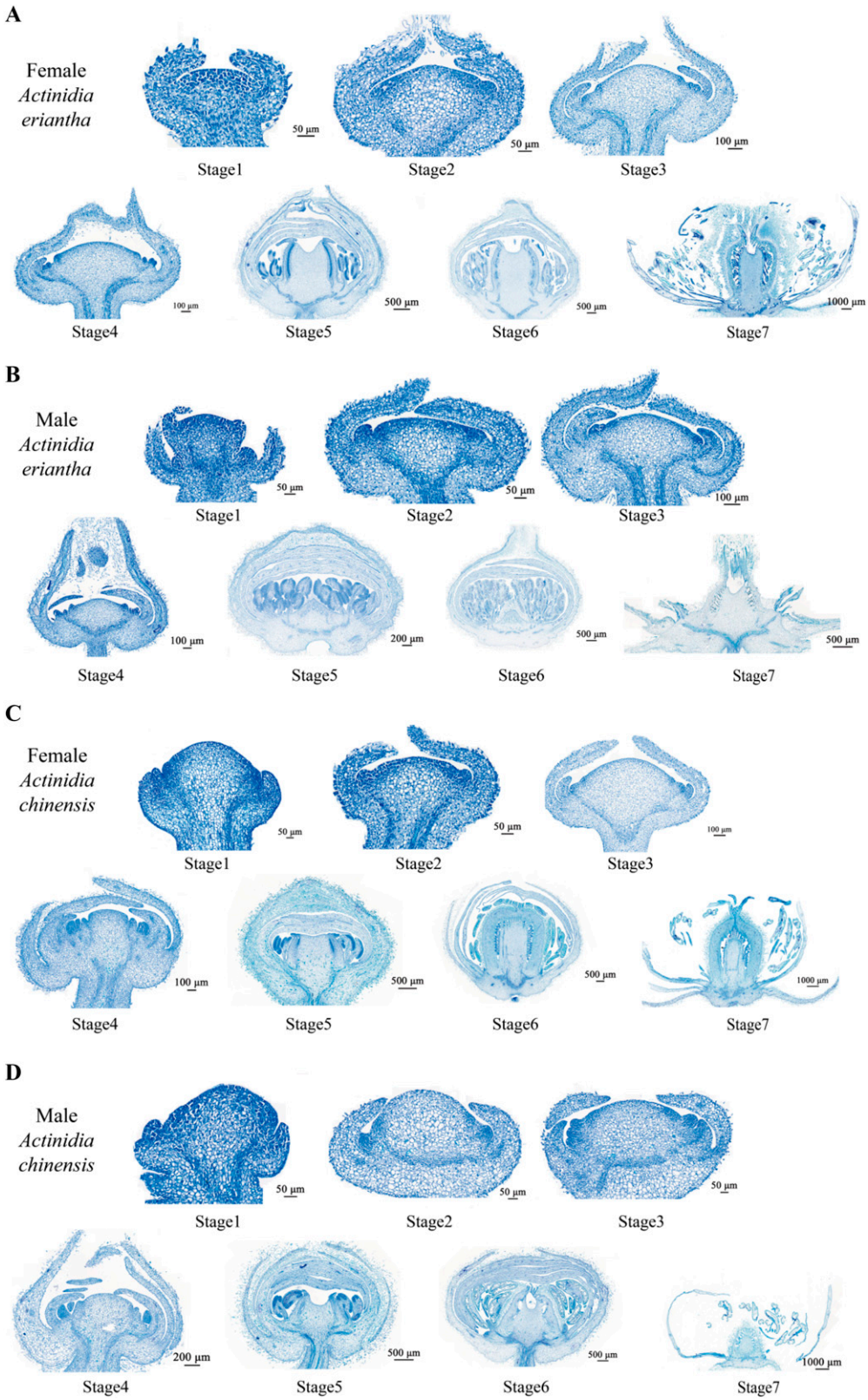

Fig. 2. Paraffin sections of seven male and female flower development stages of *Actinidia chinensis* and *Actinidia eriantha*.

The diploid male and female kiwifruits of *A. chinensis* (4-12-6 female and 2-10-2 male) and *A. eriantha* (4-4-8 female and 6-1-2 male) with consistent growth were selected as experimental materials. The sampling was conducted from Oct 2023 to May 2024.

Five flowers were randomly selected from each tree after the appearance of visible buds, and the length of the selected buds was measured every 2 d.

Paraffin sectioning. Male and female flowers of *A. chinensis* and *A. eriantha* were preserved in ice boxes and transported to the laboratory, external characteristics were observed and imaged using a motorized body microscope (SMZ25, Nikon, Japan). The flower buds were cut longitudinally with a scalpel, and some of the collected flower buds were placed in the formaldehyde–acetic acid–alcohol (FAA) fixative for more than 24 h for subsequent paraffin sectioning. The samples were transferred to 75% ethanol for 4 h and subsequently dehydrated in 85%, 90%, and 95% ethanol series and twice in 100% ethanol at

Table 2. Status of the gynoecium at each stage of development in *Actinidia chinensis* and *Actinidia eriantha*.

Stage	*A. chinensis* Female flower diam (mm)	*A. chinensis* Male flower diam (mm)	*A. eriantha* Female flower diam (mm)	*A. eriantha* Male flower diam (mm)	Female flower	Male flower
1	0.3–0.6	0.3–0.6	0.3–0.6	0.3–0.6	Sepal primordium development	
2	0.7–0.9	0.7–0.9	0.7–0.9	0.7–0.9	Petal primordium development	
3	1.0–1.5	1.0–1.5	1.0–1.5	1.0–1.5	Stamen primordium development	
4	1.6–3.5	1.6–3.5	1.6–3.0	1.6–3.0	Pistil primordium development	
5	3.6–4.5	3.6–4.0	3.1–5.0	3.1–4.5	Ovule primordia appear in the ovary	Only carpel chambers appeared, and no ovule primordia appeared
6	4.6–10.0	4.1–9.0	5.1–15.0	4.6–11.0	Ovule primordium elongation	The ovary grew slowly and no ovule appeared
7	Ovary: 5.0	Ovary: 2.3	Ovary: 5.0	Ovary: 2.7	Ovules complete development	Ovary malformation, no ovule

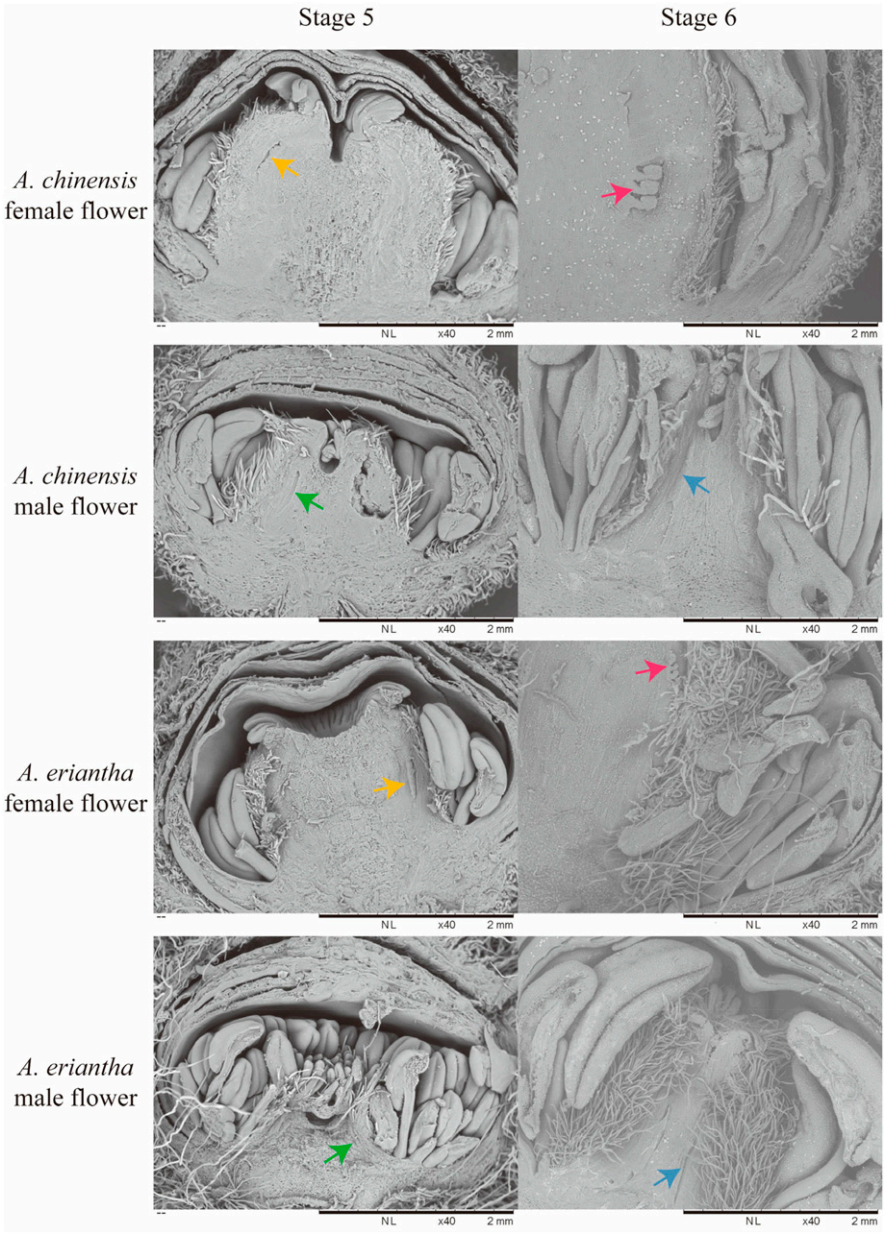

Fig. 3. SEM of female and male flowers at stages 5 and 6 in *Actinidia chinensis* and *Actinidia eriantha*. Floral developmental structures in *A. chinensis* and *A. eriantha*: yellow arrows (→) indicate the emerging ovule primordium in pistillate flowers in stage 5; red arrows (→) indicate elongating ovules in pistillate flowers in stage 6; green arrows (→) indicate the empty locule in staminate flowers in stage 5; blue arrows (→) indicate the empty locule in staminate flowers in stage 6. All images were acquired at ×40 magnification.

30-min intervals. Alcoholic benzene solution was substituted for 10 min, followed by dehydration in xylene for 10 min and dehydration in fresh xylene for 10 min. The samples were immersed in melted paraffin for 1 h at 65 °C and repeated thrice. The wax blocks were embedded using an embedding machine (JB-P5, Wuhan Junjie Electronics Co., Ltd., China). The paraffin-embedded samples were sliced using a paraffin slicer (RM2016, Shanghai Leica Instruments Co., Ltd., Germany), cut to a thickness of 4 μm, and stained with toluidine blue for 2 to 5 min. Finally, these were observed under a light microscope (Eclipse E100, Nikon) and imaged using the DS-U3 imaging system (Nikon).

Scanning electron microscopy. The bud and flower samples were soaked in 20% ethanol for 30 min to remove water from the plant tissue and subsequently transferred to 50%, 70%, 90%, 95%, and 100% ethanol for 30 min each. The dehydrated samples were dried in a carbon dioxide critical point dryer (EM CPD300, Leica) and placed in an ion sputter coater (MC1000, Hitachi, Japan) for gold plating. The material was observed and imaged using a scanning electron microscope (SEM; TM3030, Hitachi).

Pollen viability analysis. Pollen viability was assessed using an in vitro pollen germination assay. The germination medium consisted of 10% (w/v) sucrose (Sinopharm Chemical Reagent Co., Ltd., Cat. 100021418, China), 0.01% (w/v) boric acid (H_3BO_3) (Sinopharm Chemical Reagent Co., Ltd., Cat. 10004818), and 1% (w/v) agar (DingGuo, Cat. DH010-1.1, China), prepared in ddH_2O. The pollen tube germination medium was placed in the middle of the slide, a certain amount of pollen was dipped into a fine thread and gently flicked to spread the pollen evenly on the surface of the medium, which was repeated thrice. The pollen-stained slide was placed in a petri dish with a moist paper towel, and the petri dish was placed in a thermostat for dark incubation at 26 °C for 6 h. After 6 h, an inverted fluorescence microscope (DMi8, Leica) was used for examination and imaging. The following calculation was used:

$$\text{Pollen germination rate} = (\text{total number of germinated pollen grains}) / (\text{total number of germinated} + \text{non-germinated pollen grains}) \times 100\%$$

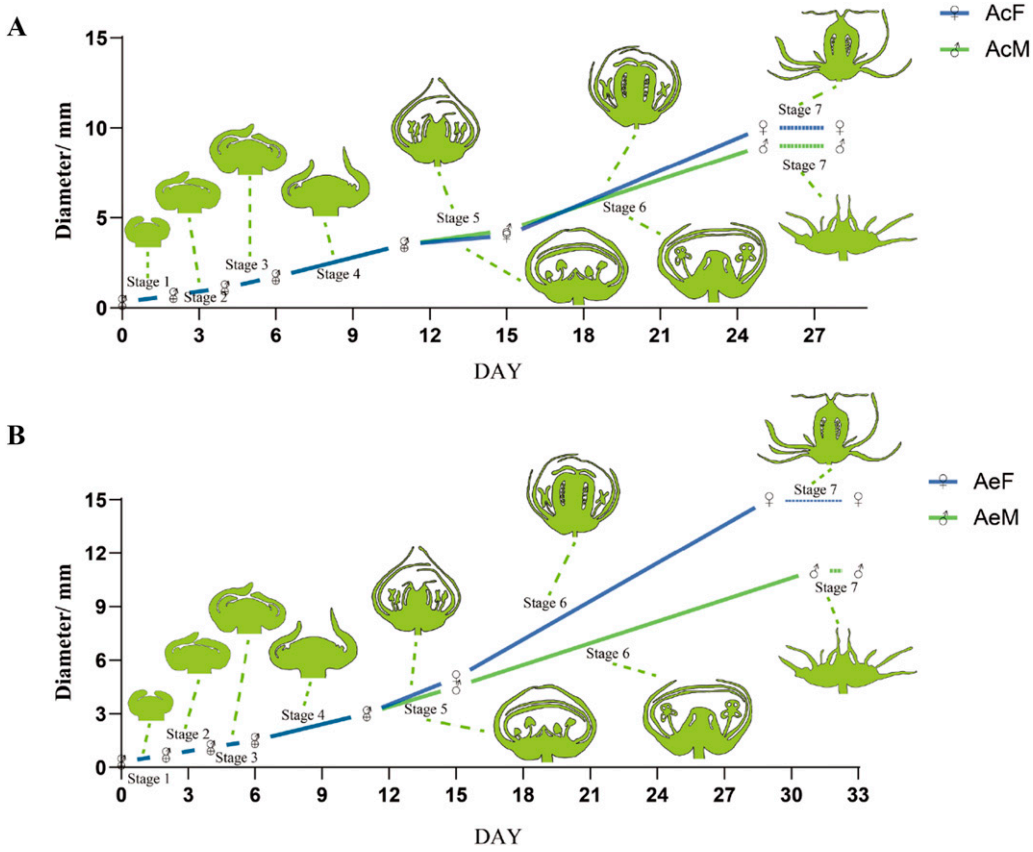

Fig. 4. Floral developmental progression in *Actinidia chinensis* (**A**) and *Actinidia eriantha* (**B**). The x-axis indicates days of development. The y-axis represents the floral bud diameter. Data series: AcF = female *A. chinensis*; AcM = male *A. chinensis*; AeF = female *A. eriantha*; AeM = male *A. eriantha*.

qRT-PCR. The total RNA was extracted using the RNAprep Pure Plant Plus Kit (TianGen, China) according to the kit instructions. The quantity and quality of RNA were determined by taking the readings on a spectrophotometer at 260/280 optical density (OD) and 1% agarose gel, respectively. The cDNA was synthesized using the PrimeScriptTM FAST RT reagent Kit with gDNA Eraser (Takara, Japan). The primers of the genes are listed in Table 1. Real-time polymerase chain reaction (PCR) was conducted in QuantStudio 6 Flex (Thermo Fisher, USA) using a ChamQ Blue Universal SYBR qPCR Master Mix Kit (Vazyme, China). A quantitative reverse transcriptase (qRT)-PCR reaction was performed according to the kit instructions. *Actin* was used as the housekeeping gene for the quantification of gene expression. The presence of a single peak in the qRT-PCR melting curve products confirmed the accuracy of the peak as well as the lack of dimers.

Results

Morphological characterization of *A. chinensis* and *A. eriantha* flowering. The flower buds of the kiwifruit were mixed buds, the sprout was full, and the scales were tightly wrapped. Morphological changes during the floral development of *A. chinensis* and *A. eriantha* were observed and imaged regularly (Fig. 1). The microstructure of buds was studied using paraffin-embedded sections. The overwintering buds of *A. chinensis* and *A. eriantha* were tightly wrapped in the xylem tissue at the base of the petiole and remained dormant until the beginning of March. The budbreak of *A. chinensis* and *A. eriantha* flower begins in early March, during which the scales surrounding the outer part of the buds expand, gradually revealing green leaf tissues. About 5 d later, the kiwifruit enters the flower bud stage, when the flower buds are inserted into the leaf axils of new short shoots. The flower bud stage of the *A. chinensis* flower lasts ~3 weeks, whereas that of *A. eriantha* lasts ~4 weeks. Subsequently, the sepals surrounding the buds split, and the petals appear at the top of the buds, entering the LuBai stage (phenological phase). Approximately 5 d later, the kiwifruit enters the efflorescence stage. A comparative phenological analysis revealed protandry in kiwifruit, with male plants initiating the development of anthesis earlier than female conspecific. A comparison of the phenological periods of *A. chinensis* and *A. eriantha* revealed no significant difference in the duration of the phenological period before the bud stage between the two kiwifruit species. However, the duration of the bud stage was longer in *A. eriantha*, and the diameter of the buds was larger than those of *A. chinensis*.

Internal morphology of male and female kiwifruit flowers. Flower buds of different diameters and sizes were collected while observing the phenological stages of *A. chinensis* and *A. eriantha* and studied using paraffin-embedded sections (Fig. 2 and Table 2). The developmental stages of male and female kiwifruit flowers are divided into seven stages, with sepal development as the initiating stage. Kiwifruit flower bud differentiation began at the outermost sepal primordium in the floral meristem (stage 1), during which the length of flower buds was ~500 μm. Subsequently, the petal primordium, which is the second most peripheral part of the floral meristem, begins to differentiate (stage 2), the length of the flower bud was ~1000 μm. This is followed by the initiation of stamen primordium differentiation (stage 3) and the beginning of pistil primordium differentiation (stage 4). The first five stages are common to both male and female kiwifruit plants; however, the pistil primordium develops more rapidly in females and more slowly in males after the onset of stage 4. Stage 5 begins with the appearance of a ventricle for ovule attachment in the gynoecium of kiwifruit flower buds (stage 5). The ovule primordium subsequently appears in the ventricle of the female kiwifruit and gradually develops into an ovule, whereas no ovule is ever produced in the ventricle of the male kiwifruit (stage 6). Finally, the kiwifruit sepals are completely dehiscent, and the petals open in stage 7. The difference between male and female flowers is primarily in stage 6, when the ovary is larger and ovules are present in female flowers, whereas the ovary in male flowers displays delayed development with an absence of ovules. No dimorphic differences between male and female flowers were observed in either *A. chinensis* or *A. eriantha* during the first five

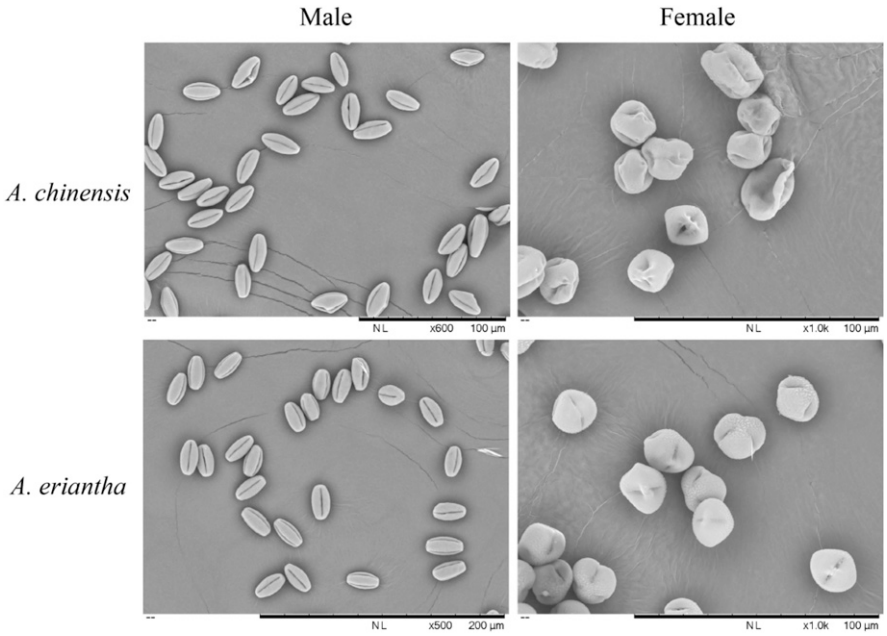

Fig. 5. Scanning electron microscopy of mature pollen between male and female plants of *Actinidia chinensis* and *Actinidia eriantha*.

developmental stages (stages 1 to 5). However, differentiation became more pronounced at stage 6. In *A. chinensis*, both male and female flowers progressed through stage 6 rapidly, completing it within ~10 d, with minimal differences in developmental timing and flower bud diameter between the sexes. In contrast, *A. eriantha* exhibited a prolonged stage 6 duration of ~15 d, accompanied by marked intersexual differences in both developmental timing and bud diameter. At stage 7, ovarian differentiation further highlighted differences: Mature ovaries of female flowers reached comparable diameters (~5 mm) in both species. Male flowers displayed species-specific variation in malformed ovary dimensions: rudimentary ovaries in *A. chinensis* were slightly smaller than those in *A. eriantha*.

We identified stage 5 as the critical period for the observed difference in gynoecium development between male and female kiwifruit flowers. Therefore, we conducted SEM using stages 5 and 6 of male and female flowers of *A. chinensis* and *A. eriantha*; the results demonstrated that at stage 5, the ovary appeared as a chamber for the appearance of ovules, and at this time the ovary in male flowers was smaller than the ovary in female flowers. At stage 6, elongated ovules appeared in the ovary of female kiwifruit flowers, whereas no elongated ovules appeared in male flowers with malformed ovaries (Fig. 3).

The diameter of kiwifruit flower buds and their timing were counted (Fig. 4), with stage 1 appearing as day 0. The androecium began to differentiate ~5 d after the sepals and petals began to develop in both *A. chinensis* and *A. eriantha*, whereas the gynoecium began to differentiate 2 or 3 d after the androecium. After about a week, *A. chinensis* flower buds stopped expanding and entered the flowering stage, whereas stage 6 of *A. eriantha* lasted for ~20 d before entering the flowering stage.

Combined with the kiwifruit's phenological stage, the flower buds had completed sepal primordial differentiation (stage 1), petal primordial differentiation (stage 2), and stamen primordial differentiation (stage 3) during the bud bursting stage and were in the process of gynoecium primordial differentiation (stage 4). When the kiwifruit was in the squaring stage, the gynoecium primordial differentiation (stage 4) was completed first within 3 d after the squaring stage. At 3 d after the squaring stage (DAS), the inner chamber of the ovary began to develop (stage 5), at which time the diameter of the flower bud was ~3.6 mm. Ovule primordia in the ovary began to elongate at 7 DAS (stage 6), when the diameter of flower buds in *A. chinensis* was ~4.1 to 4.6 mm and ~4.6 to 5.1 mm in *A. eriantha*. *A. chinensis* entered the LuBai stage when male flowers were 6 mm in diameter (~12 DAS) and female flowers were 8 mm in diameter (about 13 DAS), and *A. eriantha* entered the LuBai stage when male flowers were 8 mm in diameter (about 16 DAS) and female flowers were 12 mm in diameter (about 17 DAS). Kiwifruit flowers entered stage 7 ~4 d after the LuBai stage.

Pollen morphology and pollen fertility. SEM was used to investigate the morphological differences in the mature pollen between male and female plants of *A. chinensis* and *A. eriantha*. The pollen grains of the two kiwifruit species were monad, with subtle morphological differences. The pollen grains were prolate in the equatorial view, whereas they were trifid circular in the polar view. Pollen grains from male *A. chinensis* were perprolate, whereas those from male *A. eriantha* were prolate. Female kiwifruit pollen grains were subspheroidal (Fig. 5). In addition, a pollen viability test revealed that the pollen viabilities of male *A. eriantha* and *A. chinensis* were 48.5% and 53.6%, respectively, whereas no viable pollen was detected in female flowers (Fig. 6).

Expression patterns of sex-determining genes at different developmental stages. Male flower buds and dormant bud points of *A. chinensis* and *A. eriantha* were selected at different periods. The expression patterns of *FrBy* and *SyGl* at different periods were analyzed by real-time quantitative fluorescence PCR. Both *A. chinensis* and *A. eriantha* did not display any expression of *FrBy* and *SyGl* during the dormant period. FrBy expression was detected from stage 2 in kiwifruit buds, with sustained high levels observed beyond stage 6 in *A. chinensis*, while in *A. eriantha*, high expression was maintained beginning from stage 5. *SyGl* expression began at stage 3 in kiwifruit, with strong expression evident from stage 4 in both *A. chinensis* and *A. eriantha* (Fig. 7).

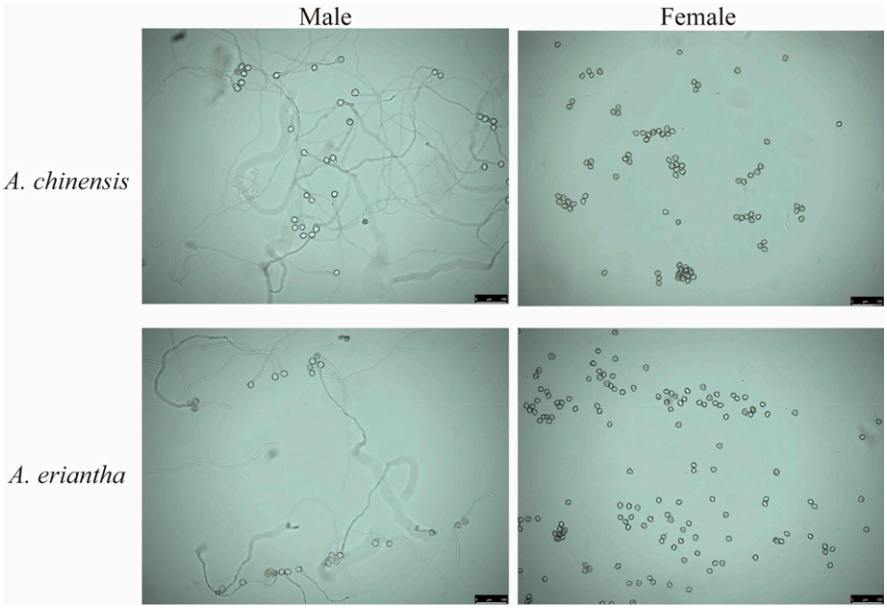

Fig. 6. Pollen tube germination in female and male flowers of *Actinidia chinensis* and *Actinidia eriantha*.

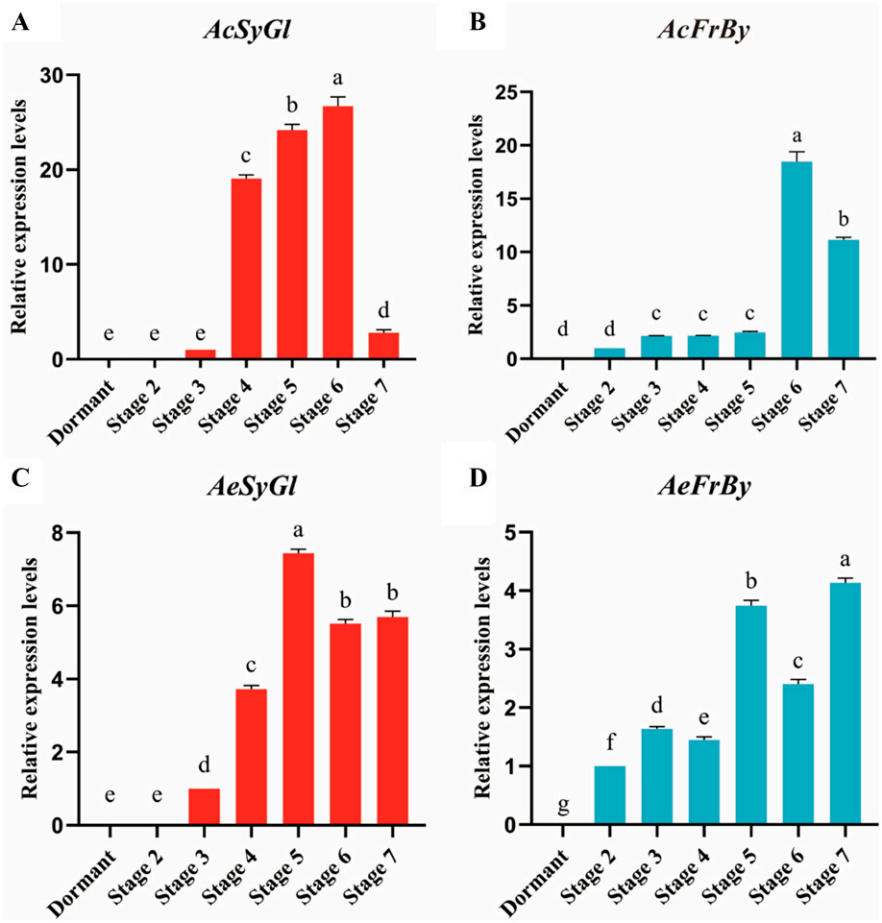

Fig. 7. Relative expression of two sex-determining genes in male kiwifruit flower buds at different stages. The relative expression of *SyGl* (**A**) and *FrBy* (**B**) in *Actinidia chinensis*, the relative expression of *SyGl* (**C**) and *FrBy* (**D**) in *Actinidia eriantha*. Letters denote significant differences [one-way analysis of variance (ANOVA), $P < 0.05$; Tukey's honestly significant difference post hoc, $\alpha = 0.05$; $n = 3$ biological replicates] among different stages.

Discussion

We sectioned and observed male and female kiwifruit flower buds of different diameters and classified the development of kiwifruit flower into seven stages (Table 2). Consistent with the findings in *A. kolomikta* and *A. deliciosa*, morphological differentiation of flower buds in *A. chinensis* and *A. eriantha* proceeds in the order of calyx, petal, stamen, and pistil, sequentially from the outside to the inside (Liu 1997; Wang et al. 2001). Consistent with previous studies on the developmental differences between male and female flowers in kiwifruit (Caporali et al. 2019; Xu 1989), we observed that both male and female stamens were present at the initial stages of flower bud development in both sexes. Divergence in floral development became apparent following pistil formation, marked by the presence or absence of ovule primordia in the ovaries of female and male flowers, respectively (Figs. 2 and 3).

After stage 5, ovule primordia appeared in female kiwifruit flowers, whereas no ovule primordia appeared in the ovary of male flowers. The ovary length in female flowers of *A. chinensis* var. "4-12-6" was ~5 mm after the complete development of male and female kiwifruit flowers, whereas it was about 2.5 mm in male flowers of *A. chinensis* var. "2-10-2." Caporali et al. (2019) reported that the ovary length in female *A. chinensis* var. "A54.20" and male *A. chinensis* var. "A54.19" were 5.5 mm and 3.5 mm, respectively, which could be attributed to the selection of different varieties of *A. chinensis*. The female *A. eriantha* "4-4-8" buds were up to 15 mm in diameter and had an ovary length of 5 mm, whereas the male *A. eriantha* "6-1-2" buds were ~11 mm in diameter and had an ovary length of 2.7 mm. *A. chinensis* and *A. eriantha* had similar ovary lengths despite the large difference in their bud diameters; this could be more indumentum in *A. eriantha*, which is shorter and less on the ovary of *A. chinensis* at stage 6, and more on the ovary of *A. eriantha* (Fig. 3). Conventional sampling standard based on single indicators (e.g., floral bud diameter, days after bud emergence) suffer from certain limitations, as our study revealed interspecific and intraspecific variations in floral developmental and morphological characteristics. We systematically investigated floral development in both male and female individuals of *A. chinensis* and *A. eriantha* and established preliminary sampling standards by integrating morphological differentiation of flower buds with phenological phases (Fig. 4). This integrated approach will provide a foundational framework for future studies on floral development in *A. chinensis* and *A. eriantha*.

We next determined the relationship between the morphological differentiation of flowering organs and phenological period in *A. deliciosa*. Xu (1989) demonstrated that the sepal primordium began to differentiate during leaf unfolding and the petal primordium, stamen primordium, and pistil primordium also started differentiating 8 d after the sepal primordium. In the present study, sepal and petal primordia began to differentiate before the visible emergence of the bud, while differentiation of the androecium and gynoecium commenced shortly after bud appearance, a process that spanned ~10 d. The observed differences in bud differentiation and phenological stages compared with previous studies may be attributed to species-specific variation in kiwifruit as well as environmental differences across years. Our study suggests that *A. chinensis* and *A. eriantha* are more likely to exhibit protandrous characteristics, while Li et al. (2024) reported that male flower differentiation slightly lags behind female flower in *A. arguta* based on external morphology. Nevertheless, in *A. arguta*, *A. chinensis* and A. eriantha, the morphogenesis of male and female flowers showed consistency in development patterns.

We focused on the similarities and differences in carpel development between male and female kiwifruit flowers. FrBy belongs to the fasciclin-like arabinogalactan family protein, and the protein functions and key structural domains are conserved (Akagi et al. 2019). Consequently, FrBy has been hypothesized to contribute to programmed degradation of tapetum cells (Akagi et al. 2019; Tan et al. 2012; Xie et al. 2022). Studies in *Arabidopsis* have demonstrated that the tapetum is not degraded during meiosis, tetrad, and uninucleate microspore stages of macrospore mother cells in *Arabidopsis*, whereas it is degraded in the bicellular pollen stage (Ariizumi and Toriyama 2011; Blackmore et al. 2007). Furthermore, Liu et al. (2018) demonstrated that the majority of flower buds of *A. chinensis* at stages III and IV (corresponding to the LuBai stage in the phenological period) were in the bicellular pollen stage. Stage 6 is speculated to be the pivotal period that contributes to the disparity in stamen development between male and female kiwifruit plants. This study posits that the degradation of the tapetum in male kiwifruit stamens at stage 6 facilitates the normal development of male pollen. Conversely, stage 6 in female kiwifruit hinders the natural programmed death of tapetum cells due to the absence of *FrBy* expression, causing abnormal pollen viability in female kiwifruit pollen. Therefore, subsequent studies may concentrate on the disparities in stage 6 between male and female flowers to further ascertain the development of kiwifruit stamens and factors leading to female kiwifruit stamen failure.

In this study, *A. chinensis* and *A. eriantha* were used as experimental materials to observe the floral cycle. *A. eriantha* flowers twice a year under optimal conditions (Walton 1995), whereas *A. chinensis* flowers only once a year. We observed no significant differences

between the two species of kiwifruit at the primary flowering stage in terms of overall phenological processes and sections at each stage of flower development. However, *A. chinensis* entered the squaring stage about 5 d earlier than *A. eriantha*, and *A. eriantha* required a longer development time at the later stage (stage 6), although ovary size at the end of flower development was not significantly different from that of *A. chinensis*. In addition, the underlying mechanisms triggering the development of secondary floral shoots in *A. eriantha* require further investigation through long-term, year-round, and phenological phase observation.

Akagi et al. (2018, 2019) used genome sequencing and transcriptome sequencing technologies and sequentially identified two kiwifruit sex-determining genes, namely, *SyGI* and *FrBy*, where *SyGI* functions as a repressor of carpel development and *FrBy* is involved in pollen development and determined that they are specifically expressed in kiwifruit male flowers. We used buds and dormant bud points of kiwifruit male flowers at different stages to detect the expression of these two genes at different times. *FrBy* was consistently and highly expressed from stage 5 or stage 6, whereas *SyGI* was consistently and highly expressed from stage 4 (Fig. 7). Therefore, stage 6 in *A. chinensis* and stage 5 in *A. eriantha* were proposed to be critical periods for male kiwifruit pollen development. The continued high expression of *SyGI* after stage 3 in kiwifruit may persistently inhibit the development of the male kiwifruit ovary, ultimately causing a small ovary and no ovule in male kiwifruit.

Conclusions

We studied the phenological stage and tissue sections of flower buds of male and female plants of *A. chinensis* and *A. eriantha* at each stage and classified the kiwifruit flower bud development into seven stages. The differences in flower development between the two species were largely in the time of entry into the squaring stage, the time taken to complete stage 6, and the size of flower buds. Differences were observed in the presence or absence of ovule elongation in stage 6, and the rate of gynoecium growth and size between the two sexes of kiwifruit. *FrBy* was highly expressed in the later stages (stage 6 in *A. chinensis* or stage 5 in *A. eriantha*) of male flower development, and *SyGI* was highly expressed in male flowers from stage 4 onward. Altogether, the findings of the present study provide a research basis for investigating male and female sex formation in kiwifruits.

References Cited

Akagi T, Henry IM, Ohtani H, Morimoto T, Beppu K, Kataoka I, Tao R. 2018. A Y-encoded suppressor of feminization arose via lineage-specific duplication of a cytokinin response regulator in kiwifruit. Plant Cell. 30(4):780–795. https://doi.org/10.1105/tpc.17.00787.

Akagi T, Pilkington SM, Varkonyi-Gasic E, Henry IM, Sugano SS, Sonoda M, Firl A, McNeilage MA, Douglas MJ, Wang TC, Rebstock R, Voogd C, Datson P, Allan AC, Beppu K, Kataoka I, Tao R. 2019. Two Y-chromosome-encoded genes determine sex in kiwifruit. Nat Plants. 5(8):801–809. https://doi.org/10.1038/s41477-019-0489-6.

Akagi T, Varkonyi-Gasic E, Shirasawa K, Catanach A, Henry IM, Mertten D, Datson P, Masuda K, Fujita N, Kuwada E, Ushijima K, Beppu K, Allan AC, Charlesworth D, Kataoka I. 2023. Recurrent neo-sex chromosome evolution in kiwifruit. Nat Plants. 9(3):393–402. https://doi.org/10.1038/s41477-023-01361-9.

Ariizumi T, Toriyama K. 2011. Genetic regulation of sporopollenin synthesis and pollen exine development. Annu Rev Plant Biol. 62:437–460. https://doi.org/10.1146/annurev-arplant-042809-112312.

Blackmore S, Wortley AH, Skvarla JJ, Skvarla JJ. 2007. Pollen wall development in flowering plants. New Phytol. 174(3):483–498. https://doi.org/10.1111/j.1469-8137.2007.02060.x.

Brundell DJ. 1975. Flower development of the chinese gooseberry (*Actinidia chinensis* Planch.). II. Development of the flower bud. N Z J Bot. 13(3):485–496. https://doi.org/10.1080/0028825X.1975.10430339.

Caporali E, Testolin R, Pierce S, Spada A. 2019. Sex change in kiwifruit (*Actinidia chinensis* Planch.): A developmental framework for the bisexual to unisexual floral transition. Plant Reprod. 32(3):323–330. https://doi.org/10.1007/s00497-019-00373-w.

Coimbra S, Torrão L, Abreu I. 2004. Programmed cell death induces male sterility in *Actinidia deliciosa* female flowers. Plant Physiol Biochem. 42(6):537–541. https://doi.org/10.1016/j.plaphy.2004.05.004.

De Mori G, Testolin R, Cipriani G. 2022. A molecular protocol for early sex discrimination (ESD) in *Actinidia* spp. J Berry Res. 12(2):249–266. https://doi.org/10.3233/JBR-211530.

Falasca G, D'Angeli S, Biasi R, Fattorini L, Matteucci M, Canini A, Altamura MM. 2013. Tapetum and middle layer control male fertility in *Actinidia deliciosa*. Ann Bot. 112(6):1045–1055. https://doi.org/10.1093/aob/mct173.

Fang JB, Zhong CH. 2019. Fruit scientific research in New China in the past 70 years: Kiwifruit [in Chinese]. J Fruit Sci. 36(10):1352–1359. https://doi.org/10.13925/j.cnki.gsxb.Z09.

Guo DD, Wang R, Fang JB, Zhong YP, Qi XJ. 2023. Development of sex-linked markers for gender identification of *Actinidia arguta*. Sci Rep. 13(1):12780. https://doi.org/10.1038/s41598-023-39561-0.

Han X, Zhang YL, Zhang Q, Ma N, Liu XY, Tao WJ, Lou ZY, Zhong CH, Deng XW, Li DW, He H. 2023. Two haplotype-resolved, gap-free genome assemblies for *Actinidia latifolia* and *Actinidia chinensis* shed light on the regulatory mechanisms of vitamin C and sucrose metabolism in kiwifruit. Mol Plant. 16(2):452–470. https://doi.org/10.1016/j.molp.2022.12.022.

Huang HW. 2016. Chapter 1: Systematics and genetic variation of *Actinidia*, p 9–44. In: Huang HW (ed). Kiwifruit. Academic Press, San Francisco, CA, USA.

Huang HW. 2022. Discovery and domestication of new fruit trees in the 21st century. Plants. 11(16):2107. https://doi.org/10.3390/plants11162107.

Li X, Shi GL, Geng JQ, Sun D, Wang ZX, Ai J. 2024. Morphogenesis, megagametogenesis, and microgametogenesis in *Actinidia arguta* flower buds. Sci Hortic. 336:113445. https://doi.org/10.1016/j.scienta.2024.113445.

Li ZJ, Liu GC. 2016. Morphologic characters of microspores and megaspores in *Actinidia arguta* during the development of floral organs [in Chinese]. Sci Silv Sin. 52(07):158–164. https://doi.org/10.11707/j.1001-7488.20160719.

Liu CY, Zhang Q, Yao XH, Zhong CH, Yan CL, Huang HW. 2016. Characterization of genome-wide simple sequence repeats and application in interspecific genetic map integration in kiwifruit. Tree Genet Genomes. 12(2):21. https://doi.org/10.1007/s11295-016-0982-2.

Liu L, Li W, Song ZJ, Song ZJ, Gao BW. 2018. Study on the relationship between bud morphology and pollen development stages in 'Donghong' kiwifruit [in Chinese]. Chin Wild Plant Resour. 37(05):30–34. https://doi.org/10.3969/j.issn.1006-9690.2018.05.008.

Liu XY. 1997. Stage of flower bud differentiation of chinese gooseberry [in Chinese]. Guizhou Agric Sci. (03):50–51.

Polito VS, Grant JA. 1984. Initiation and development of pistillate flowers in *Actinidia chinensis*. Sci Hortic. 22(4):365–371. https://doi.org/10.1016/S0304-4238(84)80008-4.

Tahir J, Crowhurst R, Deroles S, Hilario E, Deng CCL, Schaffer R, Le Lievre L, Brendolise C, Chagne D, Gardiner SE, Knaebel M, Catanach A, McCallum J, Datson P, Thomson S, Brownfield LR, Nardozza S, Pilkington SM. 2022. First chromosome-scale assembly and deep floral-bud transcriptome of a male kiwifruit. Front Genet. 13:852161. https://doi.org/10.3389/fgene.2022.852161.

Tan HX, Liang WQ, Hu JP, Zhang DB. 2012. MTR1 encodes a secretory fasciclin glycoprotein required for male reproductive development in rice. Dev Cell. 22(6):1127–1137. https://doi.org/10.1016/j.devcel.2012.04.011.

Walton EF. 1995. Occurrence of secondary floral shoots in summer on *Actinidia eriantha* Benth. N Z J Crop Hortic Sci. 23(3):341–343. https://doi.org/10.1080/01140671.1995.9513907.

Wang XD, Cang J, Wu XJ. 2001. Observation of *Actinidia kolomikta* of flower bud differentiation [in Chinese]. J Northeast Agric Univ. (03):285–289. https://doi.org/10.3969/j.issn.1005-9369.2001.03.014.

Westergaard M. 1958. The mechanism of sex determination in dioecious flowering plants. Adv Genet. 9:217–281. https://doi.org/10.1016/S0065-2660(08)60163-7.

Xie F, Vahldick H, Lin ZC, Nowack MK. 2022. Killing me softly - Programmed cell death in plant reproduction from sporogenesis to fertilization. Curr Opin Plant Biol. 69:102271. https://doi.org/10.1016/j.pbi.2022.102271.

Xu H. 1989. Differentiation and development of floral organs in *Actinidia chinensis* [in Chinese]. China Fruits. 1(63):9–12+63. https://doi.org/10.16626/j.cnki.issn1000-8047.1989.01.003.

Yang MX, Xiao DX, Liang H, Liu W. 2011. Cytomorphological observation on sex differentiation of *Actinidia chinensis* [in Chinese]. Acta Hortic Sin. 38(02):257–264. https://doi.org/10.16420/j.issn.0513-353x.2011.02.009.

Zhang Q, Liu CY, Liu YF, VanBuren R, Yao XH, Zhong CH, Huang HW. 2015. High-density interspecific genetic maps of kiwifruit and the identification of sex-specific markers. DNA Res. 22(5):367–375. https://doi.org/10.1093/dnares/dsv019.

Zhong CH, Huang WJ, Li DW, Zhang Q, Li L. 2021. Dynamic analysis of global kiwifruit industry development and fresh fruit trade [in Chinese]. China Fruits. 07:101–108. https://doi.org/10.16626/j.cnki.issn1000-8047.2021.07.025.